# JOURNAL PRE-PROOF

This is an early version of the article, published prior to copyediting, typesetting, and editorial correction. The manuscript has been accepted for publication and is now available online to ensure early dissemination, author visibility, and citation tracking prior to the formal issue publication.

It has not undergone final language verification, formatting, or technical editing by the journal's editorial team. Content is subject to change in the final Version of Record.

To differentiate this version, it is marked as "PRE-PROOF PUBLICATION" and should be cited with the provided DOI. A visible watermark on each page indicates its preliminary status.

The final version will appear in a regular issue of *Engineering Transactions*, with final metadata, layout, and pagination.

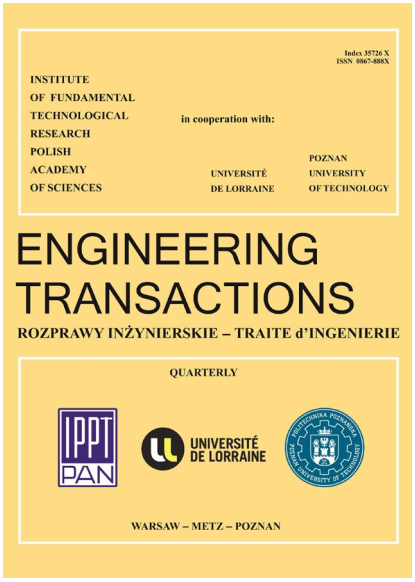


**Title:** Blade prime-number / uniform angular distribution criterion for vibration reduction

**Author(s):** Yong Li, Yaao Di, Wenzheng Dong, Fangxiang Yin, Yihao Yin, Shanling Han

**DOI:** https://doi.org/10.24423/engtrans.2025.3603

**Journal:** *Engineering Transactions*

**ISSN:** 0867-888X, e-ISSN: 2450-8071

**Publication status:** In press

**Received:** 2025-07-03

**Revised:** 2025-09-17

**Accepted:** 2025-09-18

**Published pre-proof:** 2025-12-11

**Please cite this article as:**

Li Y., Di Y., Dong W., Yin F., Yin Y., Han S., Blade prime-number / uniform angular distribution criterion for vibration reduction *Engineering Transactions*, 2025, https://doi.org/10.24423/engtrans.2025.3603

# Blade prime-number / uniform angular distribution criterion for vibration reduction

Yong Li, Yaao Di, Wenzheng Dong, Fangxiang Yin, Yihao Yin, Shanling Han*

*College of Mechanical and Electronic Engineering, Shandong University of Science and Technology, Qianwangang Road 579, Qingdao 266590, China*

**Corresponding Author e-mail: 15806673969@163.com*

Currently, the vibration noise of casting cleaning equipment exceeds 95 dB, which not only impacts the equipment's service life but also jeopardizes workers' health. The primary cause lies in the resonance tendency resulting from an uneven distribution of blades in the shot blasting device. The prime-number / uniform angular distribution criterion and the dynamic balance elimination relation are established in this paper, aiming to minimize resonance coupling while considering the internal characteristics of the shot blast device and blade assembly. Subsequently, the shot blasting device of seven prime-number angular front-curved blades was designed and established, and the dynamic balance caused by uneven blade distribution was offset by drilling. We employ discrete element method analysis to evaluate projectile velocity and stability. Results indicate that shot velocity reaches a maximum of 75 m/s with fluctuations within 4 m/s. After reaching 0.24 s, particles accelerated by the shot blasting device achieve relative stability. Finally, vibration data acquisition at a sampling frequency of 10 Ksps demonstrates that noise levels are reduced from 97 dB (traditional structure) to 93.3 dB (new model). This new criterion for shot blasting machine models mitigates vibrations during operation while enhancing working conditions and improving overall stability and reliability.

**Keywords:** shot blasting machine; vibration-induced noise; structural optimization; prime-number / uniform angular distribution criterion; shot blasting device of seven prime-number angular front curved blades.

## 1. Introduction

As a surface treatment equipment, the shot blasting machine finds extensive application across various industries. However, the operational vibration and noise issues associated with this machinery significantly impact equipment performance, personnel well-being, and environmental conditions[1].The frequency is decomposed into the fundamental frequency and its second harmonic through Fourier series[2-5]. The fundamental frequency of uniformly distributed shot blasting blades corresponds to the main frequency. Resonance occurs when either the fundamental frequency or the frequency doubling of the blade coincides with the natural frequency of the shot blasting device[6-9]. Due to the periodicity of blade rotation, the uniformly distributed blades are more prone to inducing resonance by matching the natural frequency of the system, thereby elevating the risk level.

Referring to other industries, some researchers design blades to reduce equipment noise, Luo et al. [10] discovered that a non-uniformly arranged 7-blade fan exhibits distinctive noise test results. In comparison with the uniform fan, the noise characteristics of the non-uniform fan display a broader harmonic distribution and reduced disparity between discrete and broadband noise. It is evident that incorporating non-uniform blade design offers certain advantages in vibration and noise reduction; however, prime-number angular design has only been applied in one instance within other industries, lacking a general design principle. This paper combines the design of non-uniform blades with shot blasting machines and proposes prime-number / uniform angular distribution criterion in new shot

blasters. Zhang et al. [11] analyzed the blades of shot blasting machines and found that rectangular blades can alleviate stress concentration, providing valuable insights for enhancing reliability and extending service life of these machines. Currently, although blade optimization has been conducted to mitigate stress concentration, no adjustments have been made to blade arrangement or improvements achieved regarding the noise issue associated with shot blasting machines.

The objective of this study is to provide theoretical support for optimizing the design of a shot blasting device through analysis of vibration signals and establishment of blade selection criteria. The optimization design will be conducted based on the prime-number angular distribution/uniform vibration reduction selection criterion, leading to the proposal of a shot blasting device model with shot blasting device of seven prime-number angular front curved blades. The subsequent analysis of object velocity and stability during the ejection process is conducted using the discrete element method[12]. By calculating parameters such as particle velocity changes, we can evaluate ejection stability. To address imbalance caused by uneven blade distribution, perforations will be made on the impeller disc to adjust the rotating dynamic balance of the shot blasting device. Finally, signal acquisition equipment will be used to compare vibration signals between the newly designed shot blaster and traditional ones in order to verify performance advantages of this criterion-based impeller body.

## 2. Establish prime-number / uniform angular distribution criterion for shot blast

The design of the shot blasting device not only requires blade shape improvement, but also optimization of the impeller body design to reduce resonance[13-17]. Vibration signal analysis reveals resonance between the motor and impeller body, necessitating optimization of the shot blasting device design. The key measure is to optimize the blade distribution angle and establish the prime-number / uniform angular distribution criterion of the blades: a) Calculate the desired uniform angle based on the number of blades; b) select prime-number angular positions within 1–361 to address centroid offset in blade arrangement; c) Determine a set of angles with minimal standard deviation using Eq.(1). This criterion aids in selecting mass angles close to the uniform angle, effectively enhancing system resonance frequency, reducing vibration and noise resulting from resonance, and improving mechanical equipment's operational smoothness.

The prime-number / uniform angular distribution criterion relationship is derived from the standard deviation formula:

$$S=\sqrt{\frac{\sum_{i=1}^{n}\left(wrap\left(\theta_i+\varphi\right)-\frac{360^{\circ}}{n}\cdot i\right)^2}{n}} \tag{1}$$

where, $S$ is the standard deviation; $\theta_i$ is the $i$-th prime-number angular position (in degrees); $n$ is the number of blades of shot blasting machine; $\varphi$ is the phase shift, with $\varphi\in[0°,360°/n)$. To account for the cyclic nature of $[0°,360°)$, differences are evaluated as minimum signed circular (wrapped) errors (using $wrap(x)=((x+180°)mod\ 360°)-180°$, we minimize $S$ over $\varphi$, thereby assessing uniformity with respect to an arbitrarily shifted uniform distribution.

According to the fact that the majority of existing shot blasting blades are either 6 or 8, and considering that the number of shot blasting shafts is typically 4, an imbalance in blade quantity can adversely affect both the distribution and count of smaller shafts. When there is an excessive number of small shafts, it hampers ejection efficiency; conversely, when there are too few small shafts, it compromises the strength of the shot blasting device. Accordingly, based on the prime-number / uniform angular distribution criterion of the blade, this paper opts for a specific case - seven prime-

number angular blades shot blasting device. Let $n$ be equal to 7 and substitute it into the prime-number / uniform angular distribution criterion, as per established academic standards.

Consequently, the impeller body model of the prime-number angular blades vibration damping shot blasting device was established. The utilization of prime-number angular positions reduces the risk of resonance with other components due to their unique distribution characteristics, as they do not share common factors with other numbers.

Subsequently, the impeller model of the shot blasting device was established. Since prime numbers do not share common factors with other numbers, the distribution characteristics can reduce the resonance risks with other components. According to Eq.(1), when $\varphi \in [0°, 360°/7)$, the minimum standard deviation is obtained by applying a search step size of $\Delta\varphi = 0.1°$, which enhances the precision of the result, with a longer search interval ensuring the robustness of the calculation. The results show that at $\varphi = 14.7°$, the optimal prime-numbered angular positions are 37, 89, 139, 191, 241, 293, and 347, yielding $S \approx 0.99$, the smallest standard deviation, indicating that the angular distribution of the blade positions is closest to an equidistant distribution, thus ensuring greater stability and reliability of the system.

In terms of geometric uniformity, $S$ reflects the degree of distribution uniformity, with smaller values of $S$ indicating better uniformity. However, completely equidistant distributions do not necessarily result in optimal dynamic behavior. A perfectly uniform distribution would concentrate excitation energy at the blade-passing frequency (BPF) and its harmonics, which could lead to resonance if these frequencies coincide with the system's natural frequencies. Therefore, the design criterion is not solely to minimize $S$, but to achieve minimal $S$ while ensuring that key frequency orders are shifted to avoid resonance with the system's natural frequencies, thereby optimizing the system's stability and operational reliability.

To further mitigate resonance risks, a resonance risk index, $R(\Theta)$, was introduced to assess the relative relationship between the blade frequencies and the system's natural frequencies. The resonance risk index is calculated as follows:

$$R(\Theta) = \max_{h \in \mathrm{H}} \left| \frac{1}{n} \sum_{i=1}^{n} e^{jh\theta_i} \right| \tag{2}$$

In this equation, $\mathrm{H}$ represents the set of critical frequency orders corresponding to the system's natural frequencies; $h$ denotes the frequency order, where $h$=1, 2, 3, 4, 8,9 covers the basic frequency and its harmonics; $\theta_i$ represents the angular position of the $i$-th blade.

$R(\Theta)$ represents the resonance risk index, reflecting the relationship between the excitation frequency of the blades and the system's natural frequency. The value of $R(\Theta)$ indicates the degree of difference between the excitation frequency and the system's natural frequency. A value of $R(\Theta)$ close to 0 suggests no resonance risk, while $R(\Theta)$ near 1 indicates a significant risk of resonance. The value of $R(\Theta)$ ranges from 0 to 1, with 0 meaning no resonance risk and 1 indicating a high resonance risk. If $R(\Theta)$ is less than 0.1, it indicates low resonance risk, and the system's frequency distribution is generally well aligned. Based on the above frequency analysis, we found $R(\Theta)$ =0.0736, which suggests low resonance risk and demonstrates the system's frequency alignment, thus avoiding potential resonance problems.

The generated angles are all prime-number angular positions, and since they share no common factors, their multiples do not coincide. Due to the distinct differences between prime-number values, their distribution is "uniform," avoiding synchronous resonance among the blades. For these seven blade angles $\theta_1, \theta_2, \theta_3, \ldots, \theta_7$ their relationship is defined by Eq.(3). If $\Delta\theta$ is a fixed value (e.g., uniformly distributed angles), the motion periods of the blades would synchronize, leading to resonance. However, if the angles are prime-number angular positions (such as 37°, 89°, etc.), the multiples of these angular values will not overlap within the same cycle, thereby preventing resonance.

$$\theta_i = \theta_1 + i \cdot \Delta\theta (i = 1,2,\ldots,7) \tag{3}$$

where $\theta_i$ is the angle of the $i$-th blade.; $\Delta\theta$ is the angular difference between adjacent blades.

In rotating machinery, the angular distribution of blades is directly related to their vibration modes and frequencies. Each blade's angle can be considered a vibration source linked to the rotational period. If the angular intervals between blades follow a regular pattern, vibrations from all blades may synchronize at specific rotational frequencies, leading to resonance. In contrast, a prime-number angular distribution effectively avoids such synchronization. Due to the inherent disparity between prime numbers—such as their lack of common factors—their multiples do not align within the same rotational cycle. Consequently, blades positioned at distinct prime-number angular positions exhibit differentiated rotational frequencies, thereby suppressing resonance.

As shown in Table 1 , the parameters of the shot blasting machine during operation are listed. All blades are made of high-chromium cast iron and have uniform dimensions.

**Table 1** Material parameters for different components

| name | argument | Numerical value |
|---|---|---|
| Steel pellet (cast steel) | Poisson's ratio | 0.3 |
| | Density /(kg/m$^3$) | 7.8×10$^3$ |
| | Shear modulus /Pa | 8×10$^{10}$ |
| Impeller body、Directional sleeve、Shot dividing wheel、Blades（All components are made of high-chromium cast iron ） | Poisson's ratio | 0.3 |
| Impeller body | Density (kg/m$^3$) | 7.8×10$^3$ |
| | Shear modulus /Pa | 7.6×10$^{10}$ |
| | Impeller body speed /rpm | 3000 |

The unbalanced quantity of the newly designed shot blasting machine is subsequently determined by employing Eq.(4), (5) and (6).The blade material utilized is high chromium cast iron, the density is $7.8\times10^3 \mathrm{kg/m^3}$, the mass is 0.0836kg. The Static equilibrium mass of the blade can be determined as 11.1796g, thus leading to a conclusive result.

$$\begin{cases} \left(m_b r_b\right)_x = -\sum_{i=1}^{n} mr \cdot \cos(\theta_i) \\ \left(m_b r_b\right)_y = -\sum_{i=1}^{n} mr \cdot \sin(\theta_i) \end{cases} \tag{4}$$

$$\alpha_b = \arctan \frac{\left(m_b r_b\right)_y}{\left(m_b r_b\right)_x} \tag{5}$$

$$m_b r_b = \sqrt{\left[\left(m_b r_b\right)_x^2 + \left(m_b r_b\right)_y^2\right]} \tag{6}$$

Where $m_b$ is the equilibrium mass; $r_b$ is the distance from the center of mass to the center; $m$ is leaf mass; $r$ is the distance from the center of mass of the distance between the blade center of mass and

the edge of the main (secondary) disk o the center; $\theta_i$ is the blade angle of shot blasting machine; $n$ is the number of blades of shot blasting machine; $\alpha_b$ is the phase Angle.

We then applied a formula to calculate the action balance of the shot blast blade. The eccentric mass for static balance was determined, and we measured the distance between the centroid of the shot blast blade and the edge of the main disk as 68mm, and from the edge of the auxiliary disk as 52.5 mm. By applying Eq.(7) and (8), we determined that dynamic balance mass for main disk was 4.890g, while that for secondary disc was found to be 6.309g.

$$m_i r_i = \frac{y_1 + y_2 - y_i}{y_1 + y_2} m_b r_b \tag{7}$$

$$m_{bi} = \frac{m_i r_i}{r_{bi}} \tag{8}$$

Where $m_i r_i$ is The blade is assigned to a mass radius product on a disc, 1 is the primary disk and 2 is the secondary disk; $y_i$ is the distance between the blade center of mass and the edge of the main (secondary) disk; $m_{bi}$ is dynamic balance mass; $r_{bi}$ is the distance from the center of mass to the center of a dynamically balanced mass.

After assembly, the impeller body is equipped with blades and subjected to unbalance detection on a dynamic balancing machine (as depicted in Fig. 1 (a) and (b)), with the machine parameters listed in Table 2. The rotational acceleration test of the impeller body is conducted using an electrical measurement system to quantify the unbalance. The obtained test results reveal that at 288°, the main disc exhibits an unbalance of 2.924 g, while the secondary disc shows an unbalance of 4.460 g at 272°; after rotation ceases, the main disc displays an unbalance of 2.918 g and the secondary disc records an unbalance of 4.520 g. Compared to the calculated results, there is a discrepancy of 1.966g in the balance mass of the main disk and 1.849g in that of the right disk. When at rest, the main disk exhibits a difference of 1.972g while the right disk shows a difference of 1.789g.

**Table 2** Dynamic balancing machine parameters

| Parameter | Value |
|---|---|
| Maximum rotor weight | 0.03–300 kg |
| Maximum rotor diameter | 100–800 mm |
| Maximum support distance | 250–2100 mm |
| Rotor shaft diameter range | 5–120 mm |
| Balancing speed range | 400–3000 rpm |
| Drive motor power | 0.05–3 HP |
| Minimum measurable imbalance | 0.01–0.1 g |
| Imbalance reduction rate | ≥95% |
| Minimum achievable specific imbalance | 0.2 g·mm/kg |
| Applicable rotor types | Motor rotors, flywheels, impeller body, etc. |

Deviations were observed between the test results of the dynamic balancing machine (e.g., residual unbalance) and theoretical values. Potential sources of error include installation accuracy, sensor calibration, and bearing clearance. During installation, minor deviations in blades and discs may compromise geometric symmetry and precise alignment, thereby affecting unbalance measurement. Calibration errors in sensors and environmental factors could also alter sensitivity, leading to inaccuracies in test results. Excessive bearing clearance might distort vibration signals, further impacting unbalance calculations. Despite these deviations, repeated tests demonstrated consistency with minor errors, indicating limited impact on overall conclusions. However, to ensure reliability, further optimizations are required: improving assembly precision, enhancing sensor accuracy and stability, and strictly controlling environmental conditions. Additional error analysis and refined methodologies will enhance result accuracy, ensuring the scientific validity and effectiveness of the shot blasting machine design optimization.

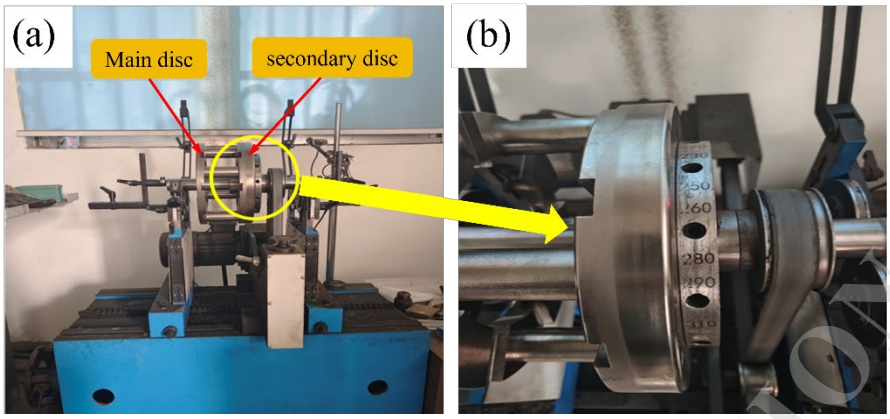


**Fig. 1** (a) Conduct imbalance detection on the impeller body using a dynamic balancing machine; (b) Utilize an angle indicator on the dynamic balancing machine.

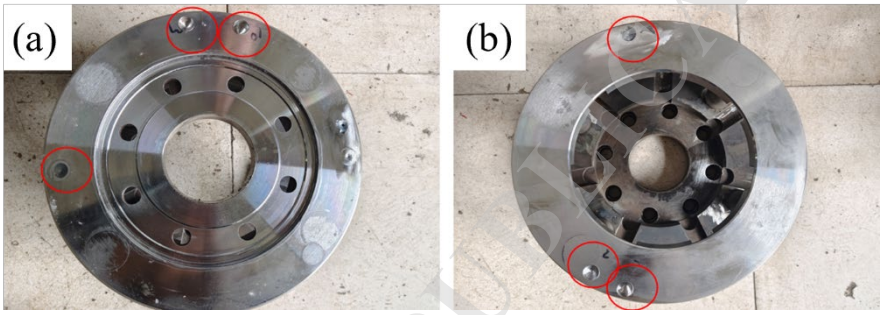


**Fig. 2** (a) Evaluate the primary disc of the impeller body following dynamic balancing; (b) Examine the auxiliary disc of the impeller body post-dynamic balancing.

According to the national standard, the unbalance should be less than 1.297 g; therefore, reductions were made in both the main disc and secondary disc of the impeller body. While drilling for weight reduction, caution was exercised to avoid excessive loss at specific positions so as not to compromise the structural integrity and strength of the impeller body. Fig. 2 (a) and (b) illustrate the modified impeller body with red circles indicating locations where weight reduction was performed. Subsequent re-testing revealed that after drilling (as depicted in Fig. 3 (a) and (d)), the main disc exhibited an unbalance of 0.294 g at 288°, while the secondary disc showed an unbalance of 0.316 g at 272°; upon rotation cessation, these values further decreased to 0.272 g and 0.376 g respectively - all well within the controlled limit of 1.297g.

The particle velocity of the shot blasting device was subsequently analyzed using the discrete element method[18-20]. The particle velocity of the shot blasting device of seven prime-number angular front curved blades reached a maximum value of 75 m/s, with a velocity fluctuation within 4 m/s. Furthermore, the particles accelerated by the shot blasting device achieved a relatively stable state after reaching 0.24 s. Through analysis of four other shot blasting models, it was found that the ejection speed of the eight-uniform front curved blade is 74 m/s, while for the eight-uniformly distributed straight blade shot blaster and 7-uniformly distributed straight blade shot blaster, their ejection speeds were measured at 64 m/s and 69 m/s respectively. These two types exhibited lower ejection speeds and poor ejection stability. Similarly, although the 7-uniformly distributed forward-curved blade shot blaster demonstrated high ejection speed, its stability was also inadequate in comparison. In terms of overall ejection stability among these devices, it can be concluded that the shot blasting device of seven prime-number angular front curved blades outperforms others in this regard. Therefore, it is speculated that this particular device will exhibit superior cleaning efficiency during operation.

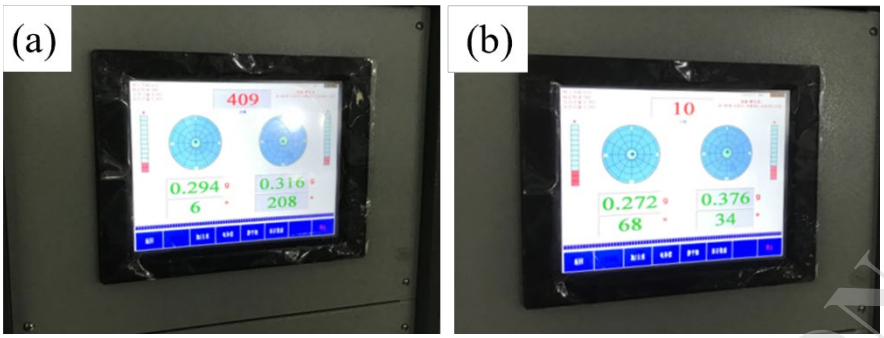


**Fig. 3** (a) Measure the residual unbalance in rotation of the impeller body after achieving balance;(b) Assess the remaining unbalance of the impeller body when it is at rest after achieving balance.

## 3. Vibration signal analysis and noise detection of shot blasting machine

In order to evaluate the resonance improvement effect and noise optimization of the new shot blasting device, a comparison was made between the frequency domain and time domain signals of the newly designed device and a traditional shot blasting device. The Hansford's HS-150 acceleration sensor was selected for measuring vibration, with data acquisition model VK701 H. Vibration data from both devices were collected at a sampling frequency of 10 Ksps, as shown in Fig. 4 and Fig. 5depicting the time domain analysis before and after optimization. Specifically, Fig. 5 (a) and (b) represent the vibration acceleration time domain diagrams of the new shot blasting device[21-24]. Analysis of the 10 Ksps vibration signal revealed significant improvement in resonance for Q034ZZ shot blaster: disappearance of octave frequencies, reduction in nine-frequency amplitude to 50% of fundamental frequency, and overall low amplitude for other frequencies; effectively controlling resonance between impeller body and motor. Both time domain and frequency domain analyses demonstrate remarkable improvement effects on the entire machine[25,26].

To mitigate the impact of random peaks, vibration intensity was quantified using the root-mean-square (RMS) acceleration within the same 2-s window. As depicted in Fig. 4 and Fig. 5, the RMS at position 1 decreased from 0.800 to 0.467 m/s² ($\Delta = 0.333$ m/s², a reduction of 41.6%), and at position 2 from 0.283 to 0.217 m/s² ($\Delta = 0.067$ m/s², a reduction of 23.5%). The reductions in RMS at both measurement points indicate effective suppression of the shot-blasting device's vibration. Thus, the struc-ture designed in accordance with the prime-number/uniform angular-distribution criterion attains a remarkable optimization effect.

In this study, the collected vibration signals are organized into groups, with each group containing 5000 data sets. Considering a sampling rate of 10 Ksps, there are a total of 20 groups. Consequently, the fast Fourier transform (FFT) is employed to convert the time domain signals into frequency domain signals, as illustrated in Fig. 6 and Fig. 7. To preserve fidelity and comparability with the raw measurements, the spectra shown are in their original form—i.e., without additional high-pass filtering or detrending; consequently, the narrow component near 0 Hz in Fig. 6 (a) arises from acquisition-chain offset/slow drift. Moreover, numerous research findings have demonstrated that FFT effectively mitigates data errors; hence it can be utilized for noise reduction applications in various data-related problems[27-30]. The Fast Fourier Transform serves as the foundation for computing the Discrete Fourier Transform (DFT).

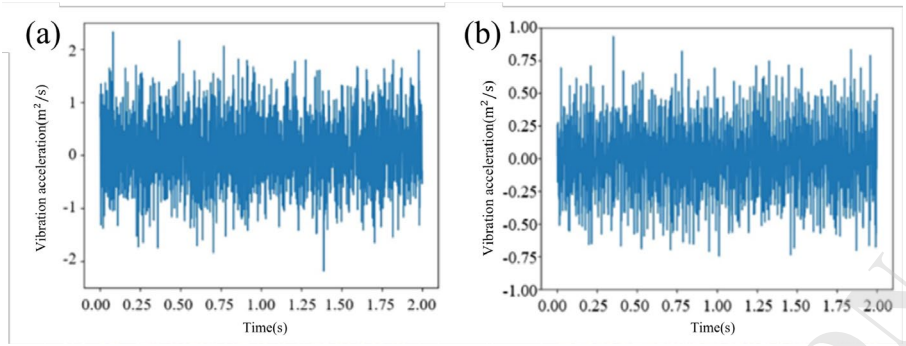


**Fig. 4** Time domain analysis: (a) Time domain diagram of position 1 before optimization; (b) Time domain diagram of position 2 before optimization.

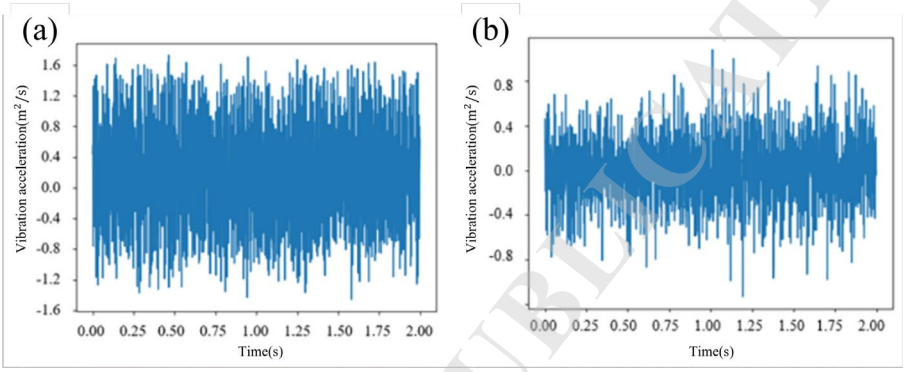


**Fig. 5** Time domain analysis: (a) Time domain diagram of position 1 after optimization; (b) Time domain diagram of optimized position 2.

The frequency domain signals before and after vibration optimization are compared and analyzed, and mark the peaks of the frequency domain signals before and after optimization with red and green circles, respectively, as depicted in Fig. 6 and Fig. 7. In Fig. 6 (a) and Fig. 7 (a) represent the frequency domain diagrams at position 1 (radial position) before and after optimization. It can be observed from the diagrams that under the load state of the shot blasting machine, the intensity of each harmonic is reduced compared to its fundamental frequency doubling. Specifically, the highest value decreases from accounting for 70% of the fundamental frequency to 50%, effectively suppressing resonance. On the other hand, in Fig. 6 (b) and Fig. 7 (b) depict the frequency domain diagrams at position 2 (axial position) before and after optimization. It can be seen that each harmonic amplitude improves following optimization with a significant reduction observed in octave frequencies - decreasing from representing 50% of their respective fundamental frequencies to approximately 20%. Furthermore, in Fig. 7 (b), it is noteworthy that only about 30% of other harmonics' highest values account for their corresponding fundamental frequencies indicating a good vibration reduction effect. Furthermore, in Fig. 6 (a) the dominant line occurs at 375-380 Hz. With $z = 7$ blades, this line corresponds to the blade-passing frequency $\mathrm{BPF} = zn/60$. Back-calculating the speed gives $n \approx 60\, f_{\mathrm{BPF}}/z \approx 3.23$ krpm. Given the frequency resolution used in this study ($\Delta f = 2\mathrm{Hz}$), the resolution-limited uncertainty is about $\pm 17$ rpm. Hence, the peak being higher than the 350 Hz expected at the nominal 3000 rpmis explained by a slightly higher actual speed, rather than an analysis artifact. The component near 50 Hz in Fig. 6(b) originates from mains/electromagnetic coupling and is unrelated to blade orders, whereas the about 430 Hz line in Fig. 6(a) is a non-integer-order response consistent with a structural or bearing-related mode of the assembly at the measured speed. Both components decrease after optimization, while the BPF-related orders exhibit the largest attenuation.

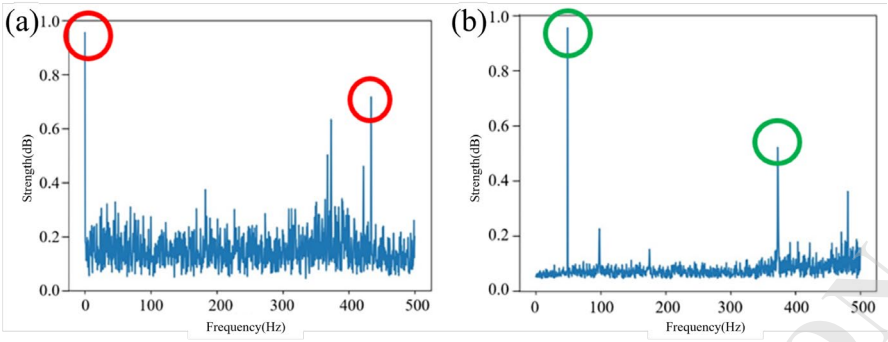


**Fig. 6** Frequency domain analysis:(a) frequency domain diagram of vibration signal at position 1 before optimization; (b) frequency domain diagram of vibration signal at position 2 before optimization.

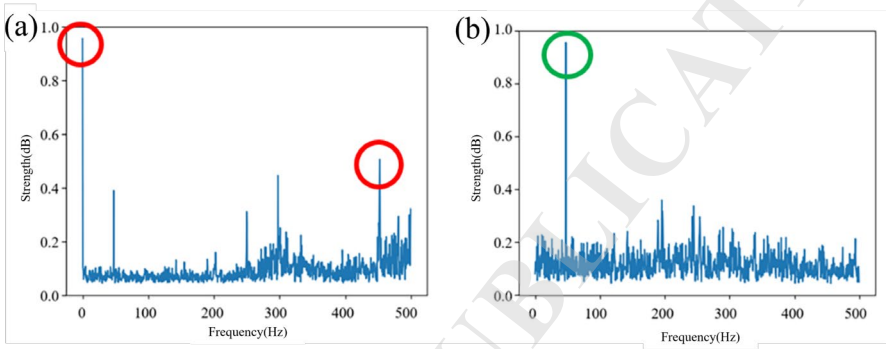


**Fig. 7** Frequency domain analysis:(a) frequency domain chart of vibration signal at position 1 after optimization; (b) frequency domain chart of vibration signal at position 2 after optimization.

The optimized impeller structure of the shot blaster has significantly contributed to reducing resonance and minimizing the acceleration value of the vibration signal, as evident from the results presented in Fig. 5 and Fig. 7. These findings not only validate the effectiveness of designing the impeller structure based on prime-number / uniform angular distribution criterion for shot blaster blades but also demonstrate its rationality. This remarkable improvement can be primarily attributed to the seven prime-number angular front curved blade's design, which effectively mitigates resonance and friction between blades, thereby reducing operational vibrations in the shot blasting machine.

The noise levels of the two shot blasters at 3000 rpm were tested, and the noise levels of the traditional Q034ZZ shot blaster and the newly designed shot blaster based on the blade prime-number / uniform angular distribution criterion were compared. The noise decibel detector of 80-130 dB is used to detect at a distance of one meter to eliminate external interference. The results show that the noise of the newly designed shot blaster is reduced by 3.7 dB, from 97 dB to 93.3 dB, which proves the effectiveness of the new design in reducing noise.

## 4. Conclusion

In this paper, a resonance coupling reduction-based optimization method is proposed to address the issue of increased vibration in the Q6919 shot blasting machine caused by motor and blade resonance. The geometric limitations of traditional impeller bodies have resulted in scarce optimization methods. This study introduces innovative prime-number / uniform angular distribution criterion and designs a shot blasting device of seven prime-number angular front curved blades based on these principles. The discrete element method is employed to analyze ejection velocity and stability, while drilling the impeller body helps reduce imbalance due to uneven blade distribution. Subsequently, projectile velocity, projectile stability, and vibration signals from the shot blasting device are explored. It can be observed that both octave frequency and nine frequency exhibit lower amplitude values compared to other frequency multiples which account for less than 50% of the fundamental

frequency; this represents significant progress when compared to traditional shot blasting devices where such amplitudes exceed 75%. These findings demonstrate the feasibility of using a seven prime-number angular curved blade shot blasting device for vibration and noise reduction purposes. In this experiment, noise detection was conducted on both the traditional structure shot blasting device as well as the shot blasting device of seven prime-number angular front curved blades resulting in a decrease from 97 dB (traditional) to 93.3 dB (seven prime-number angular), thus verifying excellent noise reduction performance achieved through design improvements.

Despite promising results, this study has certain limitations. The optimization method was primarily tested on a single type of shot blasting machine, and further validation with different configurations and operating conditions is needed. Additionally, while the seven prime-number angular blade design effectively reduces vibration and noise, its impact on other factors such as energy efficiency and longevity requires further investigation. Future research will address these aspects and extend the methodology to other machinery. Nevertheless, the design shows significant promise for applications in industries such as wind power and aerospace. As noise reduction standards tighten, the demand for this technology is expected to grow, presenting substantial potential for industrial machinery and environmental protection.

## 5. Patents

**Author Contributions:** Yong Li: conceptualization, methodology, and writing – original draft preparation. Yaao Di: methodology and writing – review and editing. Wenzheng Dong: validation, resources, and writing – review and editing. Fangxiang Yin: resources and literature survey. Yihao Yin: resources and literature survey. Shanling Han: funding acquisition, writing – review and editing, supervision, and project administration.

**Funding:** This research was funded by Natural Science Foundation of Shandong Province (Grant No. ZR2022ME118).

**Conflicts of Interest:** No potential conflict of interest was reported by the author(s).

## REFERENCES

1. Zifeng, X.; Yan, W.; Zhihai, S. Study on Noise Reduction of Q400C Shot Blasting Machine. *Modern Manufacturing Technology and Equipment* **2020**, *56*, 7-8, doi:10.16107/j.cnki.mmte.2020.0720.
2. Walker, J.S. Fourier series, Encyclopedia of Physical Science and Technology. *San Diego, CA, USA: Academic* **2002**.
3. Jenkins, W.K. Fourier series, Fourier transforms and the DFT. In *Mathematics for Circuits and Filters*; CRC Press: 2022; pp. 83-111.
4. Sundararajan, D. *Signals and systems: A practical approach*; Springer Nature: 2022.
5. Sahu, O.; Das, P.; Muni, M.K.; Pradhan, N.; Basa, B.; Sahu, S.K. Frequency-based crack effect study on beams under free vibration using finite element analysis. *Engineering Transactions* **2024**, *72*, 95-114.
6. Zhang, X.; Yan, P.; Lu, W.; Cheng, Y.; Sun, C.; Zhu, J.; Guo, W.; Cheng, X. Frequency spectrum characteristics of blast-induced vibration with electronic detonators in ground blasting. *Journal of Building Engineering* **2023**, *74*, 106892.
7. Wang, Q.; Tao, T.-j.; Jia, J.; Tian, X.-c.; Xie, C.-j. Analysis of blasting vibration duration considering frequency and energy and its application. *Heliyon* **2024**, *10*.
8. Deng, Z.; Meng, J.; Deng, Y.; Ni, J.; Ye, D. Analysis of vibration signals near ground surface during blasting excavation of a tunnel in fractured rock. *Scientific Reports* **2024**, *14*, 21909.
9. Guo, J.; Fei, H.; Yan, Y. Research and Advances in the Characteristics of Blast-Induced Vibration Frequencies. *Buildings* **2025**, *15*, 892.

10. LUO Laibin, W.Y., PENG Zhigang,OUYANG Hua. Experimental and Numerical Study on the Noise of Uneven-spaced Automobile Cooling Fans. *Noise and Vibration Control* **2021**, *41*, 175-181.
11. Zhang, Y.; Wang, S.; Pan, Y.; Zhang, T.; Jiang, Z.; Fu, X. Research on Optimization Design of Shot Blasting Machine Blade Based on Modal Analysis. In Proceedings of the 2021 Global Reliability and Prognostics and Health Management (PHM-Nanjing), 2021; pp. 1-5.
12. WU Fan ; TANG Dong-lin ; ZHAO Jiang ; WANG Bin ; LUO Xian-hui ; ZHANG Wen-wen ; Chang-zhu, G. Finite Element Analysis on Forward-Curve Blade of Shot Blasting Machine Based on ANSYS. *Mechanical Research & Application* **2015**, *28*, 27-29, doi:10.16576/j.cnki.1007-4414.2015.03.012.
13. Choi, D.; Kim, T.; Yang, C.; Nam, J.; Park, J. Discrete element method and experiments applied to a new impeller blade design for enhanced coverage and uniformity of shot blasting. *Surface and Coatings Technology* **2019**, *367*, 262-270.
14. Dan, Z.; Yuanlin, L.; Zheng, W. Noise analysis of horizontal mobile shot blasting equipment. *Journal of Heilongjiang University of Science* **2011**, *21*, 297-300.
15. Kai, Z.; Baijie, Q.; Meiru, L.; Weiqiang, G.; Jiangbo, D.; Xuefeng, C. A novel OPR-free method for blade tip timing based on adaptive variable reference blades. *Aerospace Science and Technology* **2023**, *142*.
16. Zhang, T.; Wang, S.; Yousuf, Y.A.; Jiang, Z.; Fang, J.; Fu, X.; Men, X. Study on the dynamic fatigue performance of shot blasting machine's blades based on modal analysis. In Proceedings of the Journal of Physics: Conference Series, 2021; p. 012214.
17. Wang, Y.; Sun, Z.; Liu, J.; Liu, M.; Zhou, Y. Optimization design of centrifugal impeller based on Bezier surface and FFD space grid parameterization. *PloS one* **2024**, *19*, e0310792.
18. Hou, L.; Yang, L.Y.; Wang, Y.Z.; Wang, S.R. Kinematics simulation analysis of shots in shot blasting machine based on EDEM. *Applied Mechanics and Materials* **2012**, *121*, 2071-2074.
19. LIU Yang, L.Q. Kinetic Analysis of Shot Blasting Machine with Forward Curve Blades Based on EDEM. *Machine Building & Automation* **2017**, *46*, 130-132+136, doi:10.19344/j.cnki.issn1671-5276.2017.06.036.
20. Yan, X.Y.; Wang, S.R.; Wen, D.S.; Wang, G.Q. Kinematics Simulation Analysis of Shot Blasting Projectile Based on EDEM. *DEStech Transactions on Engineering and Technology Research* **2018**.
21. Liss, M.; Martynyuk, V. Vibration analysis of shot wheel in abrasive blasting. In Proceedings of the MATEC Web of Conferences, 2023; p. 02006.
22. Yang, Z. Fault diagnosis of engine abnormal sound based on vibration analysis. *Special Purpose Vehicle* **2024**, 109-112, doi:10.19999/j.cnki.1004-0226.2024.09.027.
23. Fu, X.; Huang, K.; Sidiropoulos, N.D.; Ma, W.-K. Nonnegative matrix factorization for signal and data analytics: Identifiability, algorithms, and applications. *IEEE Signal Process. Mag.* **2019**, *36*, 59-80.
24. Yang, J.; Shi, A.; Peng, Y.; Peng, P.; Liu, J. Interface state-based bound states in continuum and below-continuum-resonance modes with high-Q factors in the rotational periodic system. *Chinese Physics B* **2024**, *33*, 084206-084206.
25. Lydakis, E.; Koss, H.; Brincker, R.; Amador, S.D.R. Data-driven sensor fault diagnosis for vibration-based structural health monitoring under ambient excitation. *Measurement* **2024**, *237*, 115232-115232.
26. Qiu, Z.; Fan, S.; Liang, H.; Liu, J. Multimodal fusion fault diagnosis method under noise interference. *Applied Acoustics* **2025**, *228*, 110301-110301.
27. Shunxi, W.; Wenjin, H. The characteristics and relationships of FT, ZT, DFS, DFT and FFT transformations. *Practical Electronics* **2015**, 121, doi:10.16589/j.cnki.cn11-3571/tn.2015.10.240.

28. Runjie, W.; Wenzhong, S.; Xianglei, L.; Zhiyuan, L. An Adaptive Cutoff Frequency Selection Approach for Fast Fourier Transform Method and Its Application into Short-Term Traffic Flow Forecasting. *ISPRS International Journal of Geo-Information* **2020**, *9*, 731-731.
29. Yang, P.; Zhou, W. Algorithmic Analysis Towards Time-Domain Extended Source Waveform Inversion. *Pure and Applied Geophysics* **2024**, 1-21.
30. Chen, Y.; Hou, L.; Lin, R.; Song, J.; Ng, T.Y.; Chen, Y. Corrigendum to "A harmonic balance method combined with dimension reduction and FFT for nonlinear dynamic simulation" [Mech. Syst. Signal Process. 221 (2024) 111758]. *Mechanical Systems and Signal Processing* **2024**, *223*, 111848-111848.